Responses of mature symbiotic nodules to the whole-plant systemic nitrogen signaling

Ilana Lambert, Marjorie Pervent, Antoine Le Quéré, Gilles Clement, Marc Tauzin, Dany Severac, Claire Benezech, Pascal Tillard, Marie-Laure Martin-Magniette, Stefano Colella, et al.

Journal of Experimental Botany, Vol. 71, No. 16 pp. 5039–5052, 2020
doi:10.1093/jxb/eraa221 Advance Access Publication 9 May 2020
This paper is available online free of all access charges (see http://jxb.oxfordjournals.org/open_access.html for further details)

RESEARCH PAPER

Responses of mature symbiotic nodules to the whole-plant systemic nitrogen signaling

Ilana Lambert[1], Marjorie Pervent[1], Antoine Le Queré[1], Gilles Clément[2], Marc Tauzin[1], Dany Severac[3], Claire Benezech[1], Pascal Tillard[4], Marie-Laure Martin-Magniette[5,6,7], Stefano Colella[1] and Marc Lepetit[1,*],

[1] Laboratoire de Symbioses Tropicales et Méditerranéennes, INRAE, IRD, CIRAD, SupAgro, Univ. Montpellier, Montpellier, France
[2] Institut Jean-Pierre Bourgin, INRAE, AgroParisTech, CNRS, Université Paris-Saclay, Versailles, France
[3] MGX, CNRS, INSERM, Univ. Montpellier, Montpellier, France
[4] Biologie et Physiologie Moléculaire des Plantes, INRAE, CNRS, SupAgro, Univ. Montpellier, Montpellier, France
[5] Institute of Plant Sciences Paris-Saclay (IPS2), Université Paris-Saclay, Univ. Evry, CNRS, INRAE, Orsay, France
[6] Institute of Plant Sciences Paris-Saclay (IPS2), Université de Paris, CNRS, INRAE, Orsay, France
[7] UMR MIA-Paris, AgroParisTech, INRAE, Université Paris-Saclay, Paris, France

* Correspondence: marc.lepetit@inrae.fr

Received 12 December 2019; Editorial decision 27 April 2020; Accepted 30 April 2020

Editors: Miriam Gifford, University of Warwick, UK

Abstract

In symbiotic root nodules of legumes, terminally differentiated rhizobia fix atmospheric N_2 producing an NH_4^+ influx that is assimilated by the plant. The plant, in return, provides photosynthates that fuel the symbiotic nitrogen acquisition. Mechanisms responsible for the adjustment of the symbiotic capacity to the plant N demand remain poorly understood. We have investigated the role of systemic signaling of whole-plant N demand on the mature N_2-fixing nodules of the model symbiotic association *Medicago truncatula*/*Sinorhizobium* using split-root systems. The whole-plant N-satiety signaling rapidly triggers reductions of both N_2 fixation and allocation of sugars to the nodule. These responses are associated with the induction of nodule senescence and the activation of plant defenses against microbes, as well as variations in sugars transport and nodule metabolism. The whole-plant N-deficit responses mirror these changes: a rapid increase of sucrose allocation in response to N-deficit is associated with a stimulation of nodule functioning and development resulting in nodule expansion in the long term. Physiological, transcriptomic, and metabolomic data together provide evidence for strong integration of symbiotic nodules into whole-plant nitrogen demand by systemic signaling and suggest roles for sugar allocation and hormones in the signaling mechanisms.

Keywords: Legumes, mature nodules, nitrogen, *Rhizobium*, sugar partitioning, symbiosis, systemic signaling.

Introduction

A hallmark trait of legumes is to form nodules with soil bacteria called rhizobia. The symbiotic root organs allow the plant to acquire nitrogen (N) from the air. In nodules, terminally differentiated bacteroids fix N_2 and supply NH_4^+ to the plant, while sucrose, synthesized in the leaves by the plant and exported to the nodules by the phloem, is the source of carbon (C) and energy fueling symbiotic N_2 fixation (SNF). NH_4^+ produced by nitrogenase is exported from the bacteroids into the cytosol of the infected cell, where it is rapidly assimilated by GS/GOGAT (glutamine synthetase/glutamate synthase) in the presence of α-ketoglutarate to synthesize amino acids that are exported outside of the nodule (mainly asparagine

in the case of *Medicago truncatula*). Efflux transporters of the SWEET family are likely to be involved in the translocation of sucrose from the phloem to the nodule (Kryvoruchko *et al.*, 2016; Sugiyama *et al.*, 2017). Once unloaded in the nodule, sucrose is generally metabolized by sucrose synthase (Baier *et al.*, 2007). UDP-glucose and free hexoses are produced, which, after phosphorylation by hexokinases, enter the glycolytic or oxidative pentose phosphate pathways and are metabolized to malate that is finally imported into the bacteroid to fuel the tricarboxylic acid (TCA) cycle (Udvardi and Day, 1997). In bacteroids, the anaplerotic 'γ-aminobutyric acid (GABA) shunt' involving pyruvate and GABA (most probably provided by the plant) has been proposed to bypass two steps of the TCA cycle by producing succinate semialdehyde, alanine, and finally succinate (Prell *et al.*, 2009). This pathway might enhance energy generation under hypoxic conditions and, therefore, might improve the efficiency of SNF (Prell *et al.*, 2009; Sulieman and Schulze, 2010; Sulieman, 2011).

The carbon metabolite cost of SNF is elevated, and the plant generally favors mineral N nutrition when the mineral N resource is not limiting plant growth. Indeed, formation of symbiotic organs requires low mineral N availability, whereas high levels of the mineral N repress SNF, inhibit nodule formation, and trigger nodule senescence (Streeter and Wong, 1988). Cysteine protease genes up-regulated in response to high nitrate concentrations are responsible for bacteroid proteolysis (Pérez Guerra *et al.*, 2010; Pierre *et al.*, 2014). Although air is an unlimited N source (air is composed of 80% N_2), plant symbiotic N acquisition is frequently spatially and/or temporally limited because nodules are highly sensitive to local environmental constraints, such as drought, that strongly inhibit SNF (Durand *et al.*, 1987; Serraj *et al.*, 1999; Gil-Quintana *et al.*, 2013). Symbiotic organs are controlled by the local N environment of the root, but also by systemic signals originating from the other organs to adjust symbiotic capacities to the N demand and the photosynthetic capacity of the whole plant. Split-root systems involving N_2-fixing *Medicago*/*Sinorhizobium* holobionts allowed characterization of these controls. The availability of a high level of mineral N was associated with the systemic repression of SNF (Ruffel *et al.*, 2008). Plant N limitation by suppressing SNF of one side of a split-root system (Ar/O_2 treatment) was associated with systemic stimulation of mature nodule growth and new nodule initiations on the other N_2-fixing roots not directly exposed to the treatment (Jeudy *et al.*, 2010; Laguerre *et al.*, 2012). This stimulation was associated with an increased allocation of photosynthates to these roots (Jeudy *et al.*, 2010). Several longstanding hypotheses to explain the modulation of SNF by the plant have been proposed. A popular model is related to the so-called 'nodule oxygen diffusion barrier' that tightly correlates with the SNF activity of mature nodules (Sheehy *et al.*, 1983; Hunt and Layzell, 1993). However whether the variations of the oxygen flux inside the nodule are the cause or the consequence of the regulation of SNF remains unclear. Another hypothesis is an 'N-feedback' inhibition of SNF by downstream N metabolites accumulated in the plant, including glutamate, asparagine, or GABA (Parsons *et al.*, 1993; Bacanamwo and Harper, 1997; Sulieman *et al.*, 2010; Sulieman and Schulze, 2010; Sulieman, 2011). The amino acid auxotrophy of bacteroids would be consistent with such control (Lodwig *et al.*, 2003). Finally, as carbon metabolites provided by the plant to the nodule are the primary nutritional source of bacteroids, a control of SNF by sucrose synthase and organic acid allocation has also been suggested (González *et al.*, 1995; Schwember *et al.*, 2019). However, the molecular mechanisms involved in these controls remain unknown, and none of these models has yet been validated. Nodule formation is under the control of the N status of the plant and the systemic repression of pre-existing nodules by the mechanism of autoregulation of nodule number (AON; Kosslak and Bohlool, 1984; reviewed by Ferguson *et al.*, 2019). Super-/hypernodulating mutants impaired in AON form nodules in the presence of a high level of mineral N, suggesting a role for this pathway in the control of nodulation by N signaling (Olsson *et al.*, 1989). Nevertheless, because the systemic response of mature nodule growth to N demand remains active in such mutants, the systemic control of mature nodules is likely to be operated by an AON-independent pathway (Jeudy *et al.*, 2010). Another pathway, acting in parallel with AON, involved in the stimulation of nodule formation in the plant under mineral N deficit has been described but it has little (if any) impact on mature nodule development (Huault *et al.*, 2014; Laffont *et al.*, 2019).

The plant transcriptional reprogramming associated with nodule formation and functioning has been characterized (El Yahyaoui *et al.*, 2004; Mitra and Long, 2004; Lohar *et al.*, 2006; Benedito *et al.*, 2008; Libault *et al.*, 2010; Moreau *et al.*, 2011; Breakspear *et al.*, 2014; Roux *et al.*, 2014). It involves the up-regulation of hundreds of specific plant genes with roles in the early signaling responses, bacterial infection, nodule formation, bacteroid differentiation, and SNF activation (Oldroyd *et al.*, 2011). These two late phases are marked by the induction of large families of genes encoding nodule-specific cysteine-rich (NCR) and glycine-rich nodule-specific peptides (GRP) associated with bacteroid differentiation (Kereszt *et al.*, 2018) as well as the genes encoding leghemoglobins allowing the bacterial nitrogenase to be active (Rutten and Poole, 2019). Bacteroid differentiation is characterized by the up-regulation of bacterial genes involved in SNF under microoxic conditions, but also by the down-regulation of an extensive number of the genes expressed in free-living cells (Becker *et al.*, 2004; Capela *et al.*, 2006). A network of plant hormones tightly regulates the symbiotic developmental program. Ethylene has been implicated in the negative control of nodule formation and nodule infection (Guinel, 2015; Reid *et al.*, 2018). Modulating shoot methyl jasmonate or cytokinin (CK) accumulation has suggested roles for these molecules in the systemic control of nodulation in *Lotus japonicus* (Nakagawa and Kawaguchi, 2006; Kinkema and Gresshoff, 2008; Sasaki *et al.*, 2014; Azarakhsh *et al.*, 2018). CLE and CEP hormone peptides have been implicated in the long-distance control of nodule formation and AON as well as in root formation and nitrate acquisition (Mortier *et al.*, 2012; Okamoto *et al.*, 2016; Taleski *et al.*, 2018; Laffont *et al.*, 2019). However, the role of these peptides in mature nodules remains poorly documented.

A few studies have shown that the addition of a high level of mineral N to the roots of the holobionts is associated with

extensive nodule transcriptome reprogramming affecting metabolism and development (Moreau *et al.*, 2011; Cabeza *et al.*, 2014). However, mineral N is a local signal by itself that is known to strongly affect the root transcriptome (Li *et al.*, 2014). These studies did not discriminate between the local effects of mineral N (i.e. at the site of application) and the systemic effects (i.e. related to the satisfaction of the whole-plant N demand). A previous report based on the analysis of split-root systems has shown that whole-plant systemic N signaling has a substantial impact on the transcriptome of whole nodulated roots, but the effects on nodule formation and/or mature nodule development could not be separated (Ruffel *et al.*, 2008). In this study, we have investigated the impact of systemic N signaling on mature N_2-fixing nodules of *M. truncatula*. We used split-root systems to investigate systemic N satiety and N deficit responses. We monitored N_2 fixation, bacteroid senescence, metabolite accumulation, and plant and bacteroid transcriptomes in order to characterize the early responses.

Materials and methods

Split-root plant growth condition

Seeds of *M. truncatula* genotype A17 were scarified in 97% H_2SO_4 for 5 min and cold-treated at 4.0 °C in water for 48 h, before germination at room temperature in the dark. After 4 d, the primary root tips were cut to promote branching of the root system. Individual plantlets were transferred into hydroponic culture tanks containing a vigorously aerated basal nutrient solution renewed every week comprising 1 mM KH_2PO_4, 1 mM $MgSO_4$, 0.25 mM $CaCl_2$, 0.25 mM K_2SO_4, 50 µM KCl, 30 µM H_3BO_3, 5 µM $MnSO_4$, 1 µM $ZnSO_4$, 1 µM $CuSO_4$, 0.7 µM $(NH_4)_6Mo_7O_{24}$, and 100 µM Na-Fe-EDTA supplemented with 1 mM KNO_3. The pH was adjusted to 5.8 with KOH. Plants were grown under 16 h light/8 h dark cycles, 250 µmol s^{-1} m^{-2} photosynthetically active radiation light intensity, 22 °C/20 °C day/night temperature, and 70% relative humidity. The 3-week-old plants were transferred to a nutrient solution adjusted to pH 7 supplemented with 0.5 mM KNO_3 containing the *Sinorhizobium medicae* md4 bacteria (10^7 cfu ml^{-1}). Nodules appeared after 4–6 d and were functional after 2 weeks. Nutrient solutions, renewed every week, were adjusted to pH 7 but not supplemented with mineral N. For split-root experiments, the root systems of 5-week-old plants were separated into two parts, each side being installed in a separate compartment. Differential N treatments were initiated that modify the N provision to one side of the root system while the other side remains supplied with aerated nutrient solution without mineral N. The N-satiety treatment (SN_2) consists of supplying the roots with a nutrient solution supplemented with 10 mM NH_4NO_3. The N-limitation treatment (DN_2) consists of removing N_2 from the treated compartment by applying a continuous flow of 80% argon/20% O_2. Nutrient solutions were changed daily after the initiation of treatments.

MD4 genome sequencing and annotation

Bacterial genomic DNA was extracted using the standard Doe Joint Genone Institute procedure. Genomic libraries were constructed with the Nextera XT DNA Library Prep Kit (Illumina). Sequencing was performed on illumina HiSeq 2500. Velvet (Zerbino and Birney, 2008), SOAPdenovo, and SOAPGapCloser (Luo *et al.*, 2012) packages were used to assemble the genome. Non-redundant contigs were ordered using the MAUVE aligner program (Darling *et al.*, 2004) utilizing the *Ensifer medicae* WSM419 genome as a reference, uploaded into the MicroScope platform, and subjected to an automatic annotation pipeline (Vallenet *et al.*, 2017). The NCBI genome sequence accession code is PRJEB29797.

RNA sequencing (RNAseq) analysis

Nodule samples (150–200 mature nodules) were collected from split-root systems described in Fig. 1A. For each condition, triplicates were collected simultaneously and separately on three plants of the same age (Fig. 1B). Treatments consist of 0 (control), 1, or 3 d of N-satiety or N-deficit. RNAs were extracted from nodules using the miRNeasy® Mini Kit (Qiagen) according to the supplier's recommendations. Plant and bacterial rRNAs were depleted using the strategy of Roux *et al.* (2014). Modified oligonucleotides used to capture rRNAs from *E. medicae* MD4 were described by Sallet *et al.* (2013) with the exception of 23S-1532-LNA that was replaced by AAG+TTAAG+CAAT+CCGTCACTA+CC ('+' preceding locked nucleotides) to match the sequence of *E. medicae* MD4. For each RNA extraction, polyadenylated plant mRNA- and rRNA-depleted total RNA libraries were generated and sequenced. They were prepared using the TruSeq Stranded mRNA Sample Preparation Kit (Illumina). Clustering and sequencing were performed in mode single-read 50 nt on illumina HiSeq 2500 according to the manufacturer's instructions, consumables, and software. The sequencing reads (ArrayExpress database accession number E-MTAB-8597) were mapped on the *M. truncatula* v4.2 and the *E. medicae* MD4 strain genomes using the glint software (T. Faraut and E. Courcelle; http://lipm-bioinfo.toulouse.inra.fr). The edgeR (v.3.22.3) Bioconductor package (Robinson *et al.*, 2010) was used for differential expression analysis in R version 3.5.1. The counts per million method was used with a threshold of one read per million in half of the samples. Libraries were normalized using the Trimmed Mean of M-values method (Robinson *et al.*, 2010; Dillies *et al.*, 2013). The differential expression analysis was applied on DN_2 and SN_2 samples separately using generalized linear models (GLMs). For each treatment (N-deficit or N-satiety), the log of the average gene expression was used as an additive function of a replicate effect and a time effect (zero time is the no treatment control). A likelihood ratio test was performed to evaluate the expression change between two consecutive times, and the probabilities of significance were adjusted using the Benjamini–Hochberg procedure. Differentially expressed genes (DEGs) were selected using an adjusted *P*-value threshold of 0.05. The robustness of the analysis was confirmed by assaying the response to N signaling of nine DEG transcripts encoding leghemoglobin, cysteine protease, and SWEET11 in nodules collected from three independent split-root experiments (Supplementary Fig. S9 at *JXB* online). The co-expression analysis was performed by the 'Coseq' (v.1.4.0) Bioconductor R package (Rau and Maugis-Rabusseau, 2018). As clustering by the Coseq algorithm may vary depending on the initialization point, the clustering was repeated 40 times, and the integrated completed likelihood (ICL) was used as a criterion to choose the best modeling of the data. MtV4 annotation was supplemented with Plant metabolic network (PMN)-Mediccyc annotation of biochemical pathways (Urbanczyk-Wochniak and Sumner, 2007). Hypergeometric tests with a *P*-value threshold of 0.05 allowed for the identification of functional enrichment in particular gene subgroups as compared with their representation in the whole genome. Plant Gene Ontology (GO) analysis was performed with the online tools AgriGO (Tian *et al.*, 2017).

Metabolomics and $^{15}N_2$ fixation

Samples (pool of the mature nodules of two plants) were collected in five replicates after 0, 1, or 4 d of N-satiety or N-deficit treatments at the same time on plants of the same age. Metabolites were extracted and analyzed by GC/MS after grinding and homogenization in liquid nitrogen as described (Fiehn, 2006; Clément *et al.*, 2018). The $^{15}N_2$ fixation activity was quantified according to Ruffel *et al.* (2008).

Histological analyses

Longitudinal sections of fresh mature nodules (70 µm thickness) were transferred to the LIVE/DEAD® solution of the BacLight™ Bacterial Viability Kit for 15 min in darkness and then incubated in calco-fluorine solution (0.1 mg ml^{-1}) for 15 min in the dark. The observations are made using a confocal fluorescence microscope (LSM 700, Zeiss).

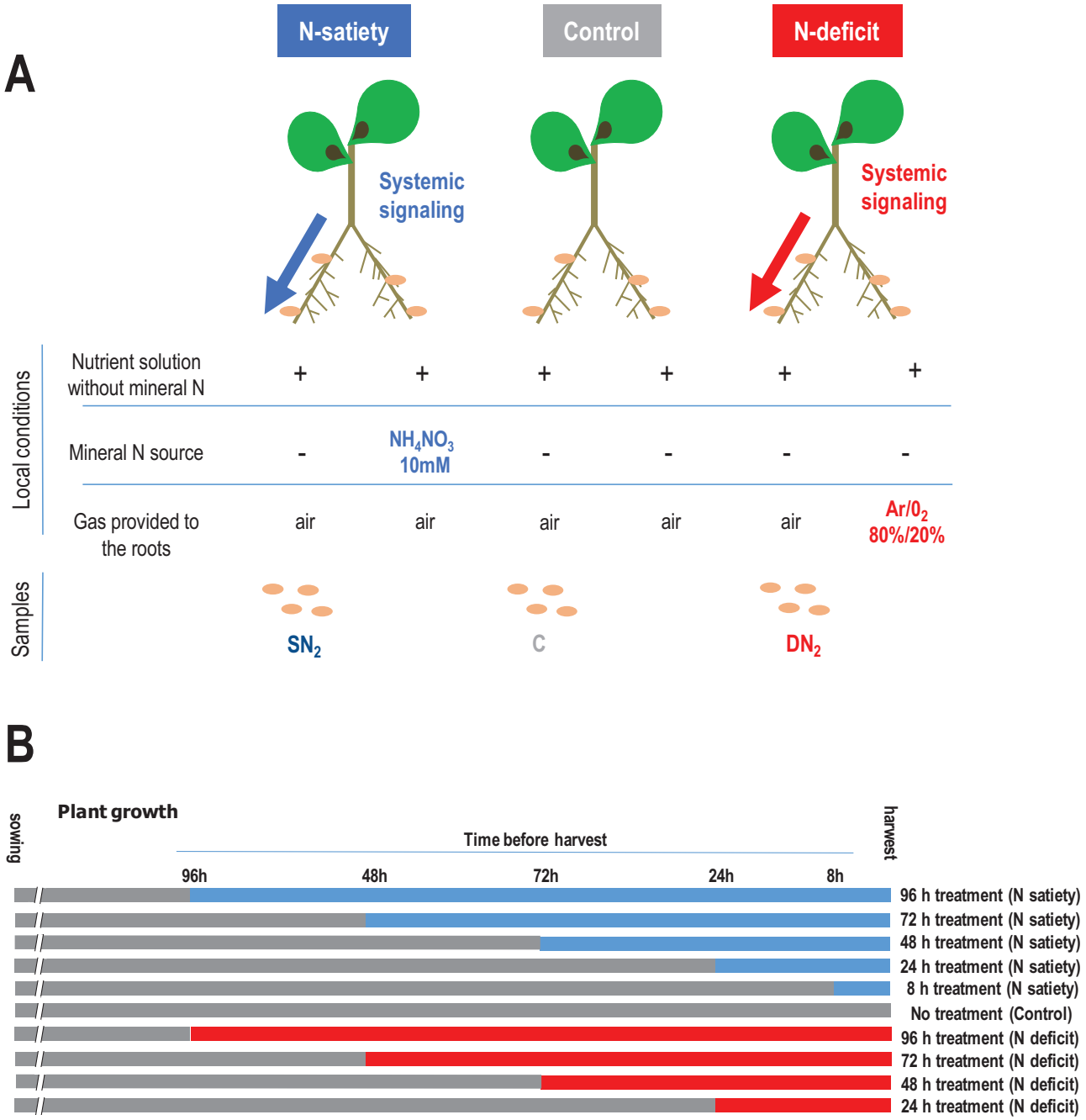

Fig. 1. Split-root systems used to study N-deficit and N-satiety signaling on the mature nodules of symbiotic plants. Plants were grown hydroponically. (A) Treatments were applied on one half of root systems and effects were studied on the other sides on the SN_2, C, DN_2, nodules of N-satiety (blue), control (gray), and N-deficit (red) plants, respectively. N-satiety treatment (blue) was achieved by providing 10 mM NH_4NO_3. N-deficit treatment (red) was achieved by replacing air by Ar/O_2 80%/20% (v/v). Control plants (gray) were not treated. The untreated roots of all plants remained normally aerated with air. (B) N-satiety, N-deficit, and control plants of the same age were harvested simultaneously. Effect of the treatments (N-satiety and N-deficit) applied during different times before harvest were compared.

Results

Split-root systems to characterize the responses of mature N_2-fixing nodules to the whole-plant N demand

Split-root systems were used to investigate the systemic control exerted by the whole-plant N status on mature nodules. Roots of individual plants carrying mature N_2-fixing nodules were separated in two compartments, and different N regimes were applied for 4 d (Fig. 1). All roots of control (C) plants were supplied with air and a nutrient solution without mineral N. 'N-satiety' plants grew in the same conditions, but a high level of mineral N (NH_4NO_3 10 mM) was provided on half of their root system. 'N-deficit' plants had half of their roots supplied with a nutrient solution without mineral N, but aerated with a gas mixture of Ar/O_2 80%/20% instead of air (suppression of the N_2 source), resulting in the immediate arrest of SNF at the site of treatment. Systemic effects of N treatment were investigated by comparing the SN_2, DN_2, and

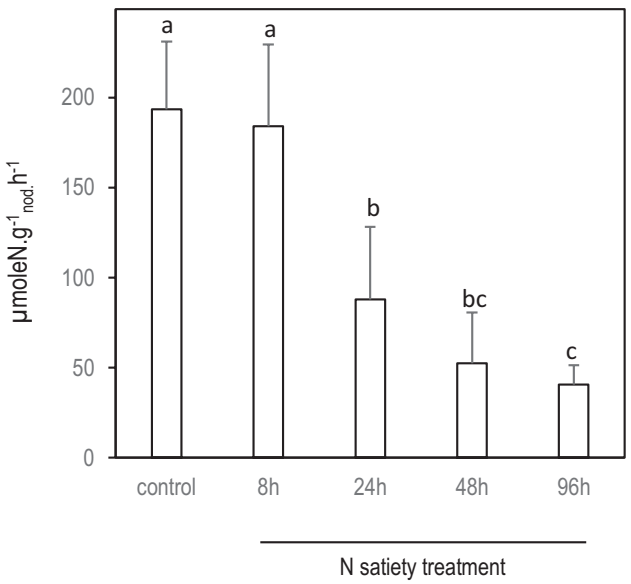

Fig. 2. Effect of systemic N-satiety signaling on the specific SNF of SN_2 mature nodules. N_2 acquisition activity per biomass of nodule was measured using $^{15}N_2$ labeling on the SN_2 nodules exposed to 8, 24, 48, and 96 h of N-satiety treatment (the detailed experimental split-root design is described in Fig. 1). Measurements are made on 8–10 nodulated root samples collected from 8–10 split-root plants. Errors bars are the SD. Kruskal–Wallis tests (significance threshold of 0.05) followed by Wilcoxon pairwise comparisons between treatments with corrections for multiple testing (significance threshold of adjusted *P*-value of 0.05) were performed. Letters indicate distinct groups of values deduced from the Wilcoxon test.

C nodulated roots (Fig. 1). SN_2, DN_2, and C nodules (Fig. 1) were in the same local condition, permissive to SNF (nutrient solution without mineral N and air), but connected to whole plants grown under 'N-satiety', 'N-deficit', and 'control' N regimes (resulting from the supply of the other side of their root system).

Systemic repression of SNF by 'N-satiety' was monitored using $^{15}N_2$ labeling after 8 h, and 1, 2, and 4 d of N treatment (Fig. 1B). We observed an extreme repression of the SNF of the SN_2 nodules between 8 h and 24 h (Fig. 2) when compared with the control nodules (Fig. 3A, B). Nodule senescence was investigated by fluorescence imaging using life/dead staining in SN_2 and DN_2 nodules after 4 d of N treatments. Systemic 'N-satiety' signaling was associated with bacteroid senescence (Fig. 3E, F), whereas a reduction of bacteroid mortality was observed in response to systemic 'N-deficit' signaling (Fig. 3C, D).

To investigate the early metabolic and transcriptional responses to systemic N signaling potentially involved in the developmental responses (i.e. nodule senescence or nodule expansion) characterized after long-term treatments, we collected nodules during the first 4 d of treatments before significant differences in biomass allocation related to treatments could be measured.

Root metabolite pool responses to systemic N signaling

Variation of soluble metabolite content associated with systemic N signaling was investigated by GC/MS analysis in C, SN_2, and DN_2 nodules after 1 d and 4 d of N treatments (Fig. 1). We detected 266 chemical species in the nodules, and we could unambiguously identify 107 of them. Most of them were soluble sugars, amino acids, and organic acids. Global soluble metabolite content varies in response to systemic N signaling: plant N-deficit stimulated their accumulation, whereas plant N-satiety decreased it (Fig. 4A).

Impacts of both N-deficit and N-satiety systemic signaling on the pool of soluble sugars in nodules were already observed after 1 d of treatment (Fig. 4B; Supplementary Table S1). N-satiety signaling was associated with a reduction of the content of sucrose, glucose, glucose 6-phosphate, fructose, and fructose 6-phosphate, and other minor sugars derived from them. Conversely, N-deficit stimulated the accumulation of these sugars in nodules. Nevertheless, levels of some minor sugars (e.g. galactose, xylose, and rhamnose) were affected to only a very small degree by the treatment, indicating that these extensive changes were not generalized to all sugars (Supplementary Table S1). Together with soluble sugar variations, we observed variations in nodule amino acid and organic acid contents (Fig. 4C, D; Supplementary Tables S2, S3). N-satiety signaling was associated with a transient stimulation of the accumulation of several of these metabolites after 1 d of treatment followed by a substantial reduction, while N-deficit stimulated their accumulation in mature nodules. Major amino acids such as asparagine, and glutamate, and minor ones such as alanine and GABA (Fig. 4C; Supplementary Table S2), displayed these variations, as did primary organic acids such as malate, pyruvate, succinate, and fumarate (Fig. 4D; Supplementary Table S3). Interestingly, succinic semialdehyde, a minor organic acid that is barely detectable in control samples and N-sufficient plants, accumulated in nodules under N-deficit (Fig. 4D; Supplementary Table S3). Together with GABA and alanine (Fig. 4C; Supplementary Table S2), they mark the stimulation of the 'GABA shunt' of the TCA cycle in response to systemic N-deficit signaling under the anaerobic conditions of mature nodules. Nonetheless, not all amino and organic acids followed these trends. Many minor nodule amino acids, such as tryptophan, valine, arginine, and isoleucine, were strongly accumulated in response to plant N-satiety and displayed only little variation under N-deficit (Fig. 4C; Supplementary Table S2). Systemic N signaling does not significantly affect citrate (the primary organic acid of the nodule) and malonate pools (Fig. 4D; Supplementary Tables S3). Altogether, these results revealed a specific impact of systemic N signaling on metabolite contents in nodules.

Global responses of the mature nodule transcriptome to systemic N signaling

The effect of systemic N signaling on the transcriptome responses of the two symbiotic partners was investigated. We used the split-root systems described in Fig. 1A. DN_2 or SN_2 nodules were collected in triplicate on N-deficit or N-satiety plants (1 d or 3 d treatments) and compared with the nodules collected from control plants (Fig. 1B). To simultaneously monitor plant and bacterial gene expression, RNAseq analysis was performed on both polyadenylated RNA- and rRNA-depleted

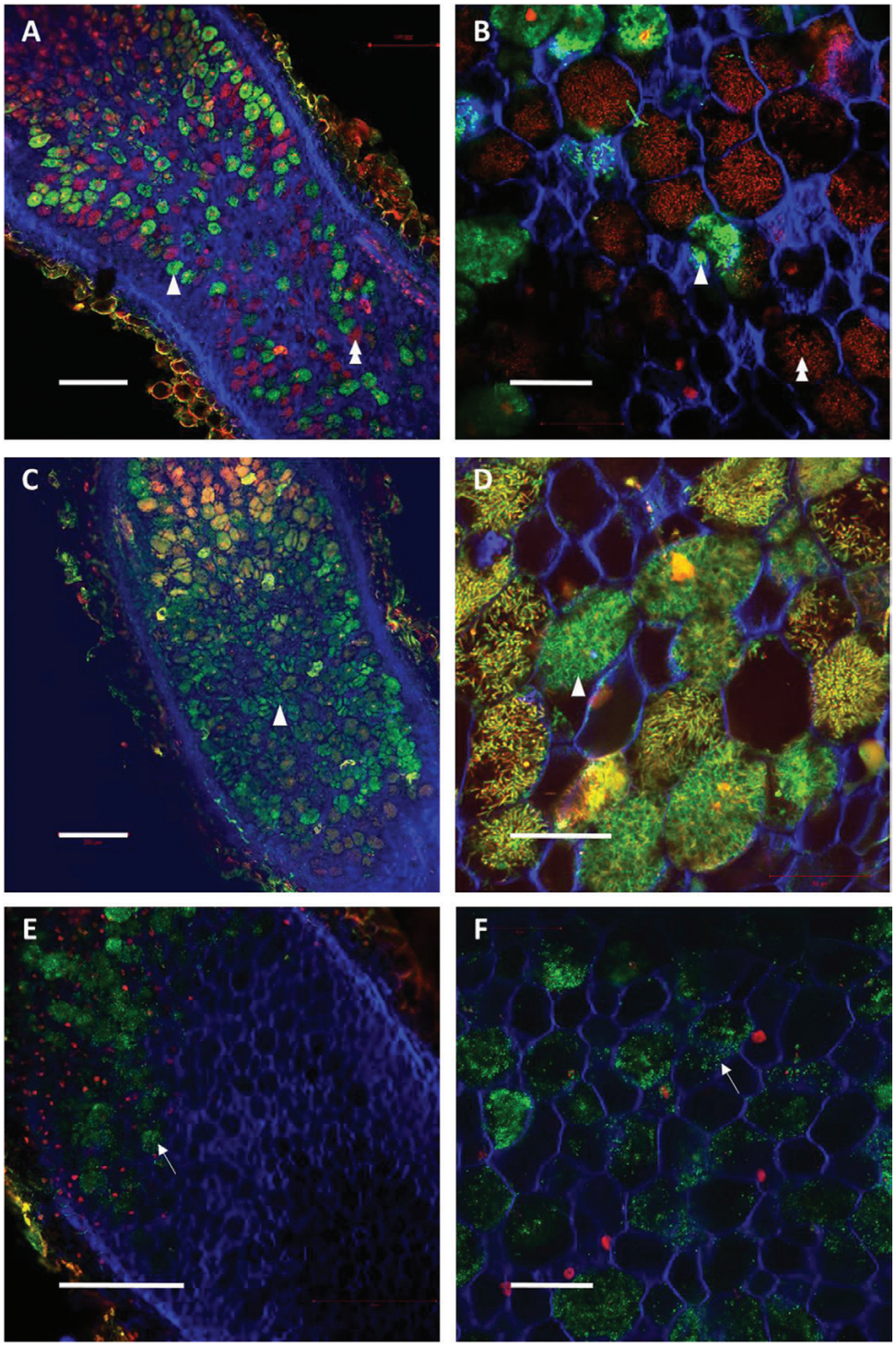

Fig. 3. Effect of systemic N-satiety signaling on the bacteroid viability of C, DN_2, and SN_2 mature nodules. N-satiety split-root plants were cultivated as described in Fig. 1 and nodules were collected after 4 d of N-satiety treatment. Confocal microscopy images of transversal sections of control (A, B), DN_2 (C, D), and SN_2 (E, F) nodules upon live/dead and calco-fluorine staining. Viable bacteroids appear green (arrowheads) and dead bacteroids red (double arrowheads) inside plant cells. Control plants contained red- and green-labeled bacteroids. In SN_2 nodules, bacteroids were almost completely destroyed, and only undifferentiated bacteria (arrows) were observable after 4 d (E, F). A higher level of green signal is found in DN_2 nodules as compared with control nodules, suggesting delayed mortality compared with control nodules. Scale bars correspond to 200 µm in (A), (C), and (E), and 50 µm in higher magnification panels (B), (D), and (F).

total RNAs. A total of 9110 plant DEGs in at least one condition (adjusted *P*-value <0.05) were identified (Supplementary Fig. S1; Supplementary Tables S4, S5). Systemic N signaling has a major impact on the nodule transcriptome as 44% of the plant genes expressed in the symbiotic organ are DEGs (39% and 13% in response to N-satiety and N-deficit, respectively). Only 5% of these genes were identified by the previous studies describing N responses of the symbiotic organs (Supplementary Fig. S2; Ruffel *et al.*, 2008; Cabeza *et al.*, 2014). Although N-deficit and N-satiety signaling targeted rather

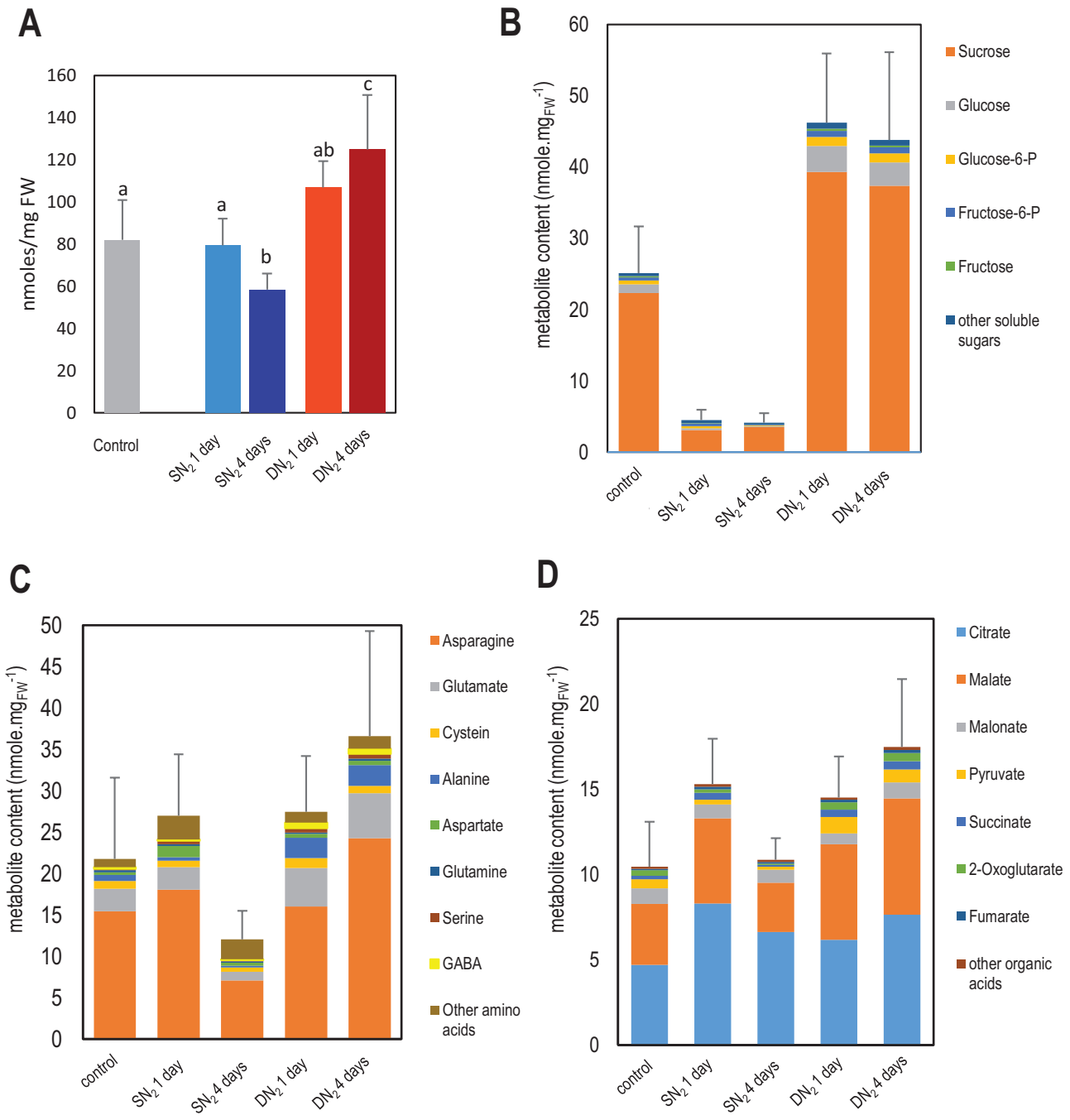

Fig. 4. Effect of systemic N signaling on mature nodule metabolite content. Analysis was performed by GC/MS. Measurements were done on five independent biological replicates (one biological replicate is 200–300 nodules of two plants). Error bars are the SDs. (A) Total metabolite content. Gray, blue, and red bars correspond, respectively, to control, SN_2, and DN_2 nodules consistently with the colors in Fig. 1. We performed Kruskal–Wallis test (0.05 significance threshold) followed by Wilcoxon pairwise comparisons between treatments with corrections for multiple testing (0.05 significance threshold of the adjusted *P*-value). Letters indicate distinct groups of values deduced from the Wilcoxon test. (B) Sugar contents. Colors correspond to the five most abundant sugars of the nodules, representing >95% of the total sugar content of the mature nodules of control plants (complete data and statistical analysis are given in Supplementary Table S1). (C) Amino acid contents. Colors correspond to the eight most abundant amino acids of the nodules representing >95% of the total amino acid content of the mature nodules of control plants (complete data and statistical analysis are given in Supplementary Table S2) (D) Organic acid contents. Colors correspond to the seven most abundant organic acids of the nodules, representing >95% of the total organic acid content of mature nodules of control plants (complete data and statistical analysis are given in Supplementary Table S3).

specific DEG groups, they also targeted a broad set of 1778 common genes (common DEGs) responding to both treatments (Supplementary Fig. S1). Total DEGs were strongly enriched with plant genes displaying responses to both treatments as compared with total expressed genes (hypergeometric test, $P<0.01$). N-satiety- and N-deficit-responsive genes display specific enrichments of some GO terms as compared with the entire transcriptome (Supplementary Table S6). Comparing these enrichments confirmed the specificities of the two systemic N responses (i.e. GO terms enriched in one group and

not in the other), but also revealed enrichments of the same functions (i.e. the same GO terms enriched in both groups). Such massive transcriptome reprogramming was not observed in bacteria as only 674 differentially accumulated bacterial transcripts were identified (Supplementary Tables S7, S8), representing 11% and 1% of the expressed bacterial genes in response to N-satiety and N-deficit, respectively. Within the few N-deficit-responsive transcripts of the bacteria, we found no clear evidence of the transcriptional activation of the 'GABA shunt' of the TCA cycle at the level of metabolite accumulation. Most of the bacterial DEGs were identified in the nodules exposed to 3 d of N-satiety treatment (Supplementary Fig. S1B). However, at this stage of the treatment, the viability of bacteroids, the main fraction of bacterial cells present in the mature nodules, was probably impaired (Fig. 3). Bacteroid death had most probably (i) reduced the overall expression level of bacterial genes (that is assumed to be stable during the treatments); and (ii) modified the relative level of viable free-living versus differentiated bacteria in the samples. Therefore, the effect of long-term N-satiety treatments on the bacterial transcriptome needs to be interpreted with caution as the changes were probably related to bacteroid death and only indirectly to N signaling.

Analysis of plant transcriptome reprogramming in response to systemic N signaling

Co-expression analysis was performed on plant DEGs to cluster genes displaying closely related responses to systemic N signaling. The procedure was able to classify 86% of total DEGs within 15 clusters (Fig. 5; Supplementary Table S9). We combined 11 clusters (representing 85% of the total plant DEGs) in two metaclusters. Metaclusters A (clusters 1, 2, 5, 11, 13, and 14) and B (clusters 3, 6, 7, 8, and 9) were formed by regrouping clusters displaying respectively up- and down-regulation responses to N-satiety signaling. Most DEGs correspond to genes expressed in the various zones of the mature nodules described by Roux *et al.* (2014) (Supplementary Table S10). The transcript accumulations of the genes belonging to the A and B metaclusters were not equivalently spatially distributed in nodules. The A and B metacluster genes were abundant in the early infection zone, but the A metacluster genes were particularly active in the N_2-fixing zone containing symbiosomes and differentiated bacteroids, whereas B metacluster transcripts were particularly abundant in the meristematic and the late infection zone (Supplementary Table S10). Enrichments of particular plant gene annotations were estimated by hypergeometric tests. The frequencies of annotations in clusters/metaclusters were compared with frequencies in the entire transcriptome to estimate whether observed enrichments were the result of chance or possibly related to a biological function (Fig. 6; Supplementary Tables S9, S11). Globally, DEGs were enriched in genes of the symbiotic-related islands (SRIs) physically clustered within the *M, truncatula* genome (Pecrix *et al.*, 2018), illustrating the strong impact of systemic N signaling on symbiosis (36% of the SRI genes were DEGs).

Metacluster A gene annotations were enriched with the keyword 'senescence'. Consistently, the transcript encoding MtNAC969 (Medtr4g081870; de Zélicourt *et al.*, 2012), a transcription factor controlling nodule senescence, was found in cluster 5. Furthermore, cluster 1 was enriched for cysteine protease transcripts involved in the proteolysis of bacteroids during nodule senescence. The corresponding transcripts were down-regulated in response to N-deficit, suggesting that they were instrumental in both N responses (Supplementary Figs S3, S4). Three genes encoding cystatin, an inhibitor of cysteine protease (van Wyk *et al.*, 2014; clusters 14, 5, and 11; Medtr3g084780, Medtr4g01762, and Medtr3g043750, respectively) were also up-regulated in response to N-satiety systemic signaling. In addition, gene annotations of the metacluster A and particularly cluster 5 were strongly enriched with keywords 'chitinase' or 'glucanase' or 'pathogenesis-related' (16 transcripts), indicating that systemic N-satiety signaling stimulated the accumulation plant transcripts related to defense responses against microorganisms. This stimulation paralleled the up-regulation of the jasmonic acid biosynthesis genes (11 transcripts in metacluster A). Nevertheless association of these functions with the response to systemic N-satiety signaling was not systematic, as other transcripts annotated as 'chitinase' or 'glucanase' or 'pathogenesis-related' were enriched in down-regulated gene clusters or clusters displaying other expression profiles (clusters 6, 4, 10, 12, and 15), suggesting that transcripts related to defense against microorganisms were contributing to several N signaling responses. Metacluster A transcripts were enriched in annotations related to CK synthesis and degradation: two-component response regulators (eight transcripts), and enzymes involved in the inactivation of CKs by glycosylation (five transcripts). The up-regulation of these transcripts in response to N-satiety parallels the repression of the accumulation of three other transcripts belonging to metacluster B encoding isopentenyl transferase (IPT; clusters 6 and 7) and CK riboside 5'-monophosphate phosphoribohydrolase (cluster 12), both involved in the biosynthesis of active CKs, but also a transcript encoding CK oxidase (cluster 7) involved in the inactivation of CKs.

Genes belonging to metacluster B were repressed by systemic N-satiety signaling. The down-regulation of the transcripts encoding leghemoglobins (clusters 6 and 7; Supplementary Fig. S5), ammonium assimilation, and L-asparagine synthesis (both pathways enriched in metacluster B) paralleled the repression of SNF. The expression of many metacluster B genes marked the repression of sugar metabolism and transport in response to systemic N-satiety systemic signaling. Transcripts related to pathways of glycolysis, gluconeogenesis, sucrose, and starch metabolism were represented in metacluster B. Metacluster B also included 11 transcripts annotated as involved in sucrose transport. Striking examples were transcripts encoding the main nodule efflux sucrose transporters, MtSWEET11 (Medtr3g098930), MtSWEET15c (Medtr7g405730), and MtSWEET12 (Medtr8g096320), that were down-regulated by N-satiety. However, enrichment in sugar transporter transcripts was found in metacluster A (namely in cluster 11; six transcripts). These transcripts were up-regulated during nodule senescence and might be involved in the remobilization of sugars from the senescent organs to the plant. Whether these different behaviors of sugar transporter transcripts are related to

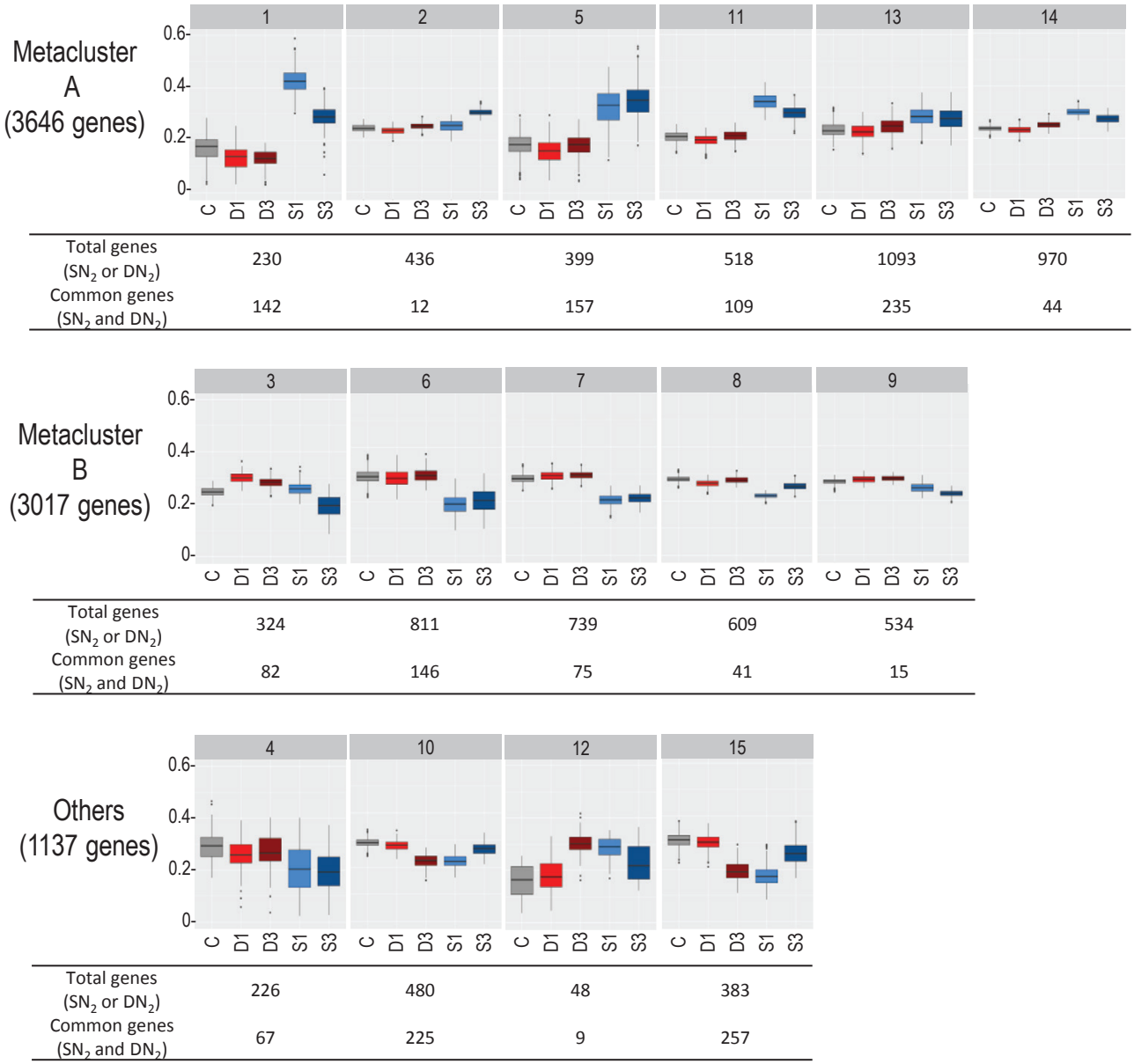

Fig. 5. Clusters and metaclusters of DEGs co-expressed in response to systemic N signaling. Normalized expression profiles of genes (relative transcript accumulations) are represented per cluster using box plots. C, D1 and D3, and S1 and S3 correspond, respectively, to control (gray), DN_2 (1 d and 3 d of N-deficit treatment in red and brown), and SN_2 (1 d and 3 d of N-satiety treatments in light and dark blue), as the samples described in Fig. 1. The total number of DEGs (i.e. differentially expressed in response to N-satiety or N-deficit) as well as the numbers of common DEGs (i.e. differentially expressed in response to N-satiety and N-deficit) of the clusters are indicated.

the direction of the sugar flux mediated by these transporters remains to be determined. Although transcripts encoding enzymes involved in ethylene biosynthesis may display different responses to systemic N signaling, this annotation was globally overenriched in metacluster B (10 transcripts). Many transcripts associated with nodule formation and/or development belong to metacluster B. Repression by N-satiety signaling of 35 core histone and 18 cyclin transcripts (enriched in metacluster B; Supplementary Tables S9, S11) were probably correlated with a reduction of nodule cell division. Metacluster B was enriched in numerous nodule-specific transcripts: 24 encoding GRP peptides (Supplementary Fig. S6), 257 encoding NCR peptides (Supplementary Fig. S8), and 20 others annotated as 'nodulins' (Supplementary Fig. S7). Two subgroups of NCR transcripts were easily discriminated based on their accumulation kinetics in response to N-satiety systemic signaling: early (before 1 d of treatment; 114 trancripts) or late (between 1 d and 3 d treatment; 101 genes) down-regulation. In addition, several key transcripts associated with flavonoid biosynthesis (overenriched in metacluster B; nine transcripts), as well as *Rhizobium* infection and nodule formation, such as MtPUB1 (Medtr5g083030), MtDMI1 (Medtr5g083030), MtLIN (Medtr1g090320), MtRPG (Medtr1g090807), MtEFD (Medtr4g008860), MtMMPL1 (Medtr5g036083), MtVPY (Medtr5g083030), MtNFY-A1 (Medtr1g056530), MtNOOT1 (Medtr7g090020), MtDME (Medtr1g492760),

Fig. 6. Enrichment in the functional annotation terms of the co-expressed DEGs as compared with their representation in the whole genome by hypergeometric tests. Red and blue colors correspond, respectively, to enriched and underenriched clusters or metaclusters (*P*-value <0.05). Complete data are given in Supplementary Table S11. [a]Mtv4.2 gene annotation term. [b]Plant Metabolic Network MedicCyc annotation term. [c]*P*-value=0.058.

MtN21 (Medtr3g012420), and MtN6 (Medtr1g062710), also belonged to metacluster B. Some of the transcripts involved in nodule development were also up-regulated by N-deficit (cluster 3); that is, most of the NCRs (including MtDNF4/NCR211; Medtr4g035705) and GRPs accumulated transcripts as well as MtDME and MtN13. Nevertheless, not all key genes of early or late nodule development are down-regulated by N-satiety signaling. For example, *MtENOD11* (Medtr3g415670), *MtNIN* (Medtr5g099060), *MtFLOT2* (Medtr3g106420), *MtSymRem* (Medtr8g097320), *MtLYK3* (Medtr5g086130), *MtRSD* (Medtr3g063220), *MtDNF2* (085800), and *MtSymCRK* (Medtr3g079850) are expressed but did not respond significantly, while *MtNSP1* (Medtr8g020840) and *MtENOD40* (Medtr8g069785) were slightly up-regulated (in metacluster A).

Finally, we paid particular attention to the 15 transcripts detected in mature nodules encoding CLE and CEP peptide hormones. A number of them were differentially accumulated in response to systemic signaling (11 CLE and two CEP transcripts; Supplementary Fig. S8). Their accumulation profiles were diverse as they are related to either metacluster A (one CEP and four CLE transcripts) or metacluster B (three CLE transcripts), or display other expression profiles (one CEP and four CLE transcripts), suggesting that they may be associated with multiple responses to systemic N signaling.

Discussion

This study shows that the whole-plant N status triggers systemic signaling impacting mature nodule functioning and development associated with massive metabolic changes and transcriptome reprogramming(s).

The whole-plant N-satiety treatment results in the systemic repression of SNF. This down-regulation occurs within hours after providing a high level of mineral N to the treated side of the split-root system (Fig. 2) and is correlated with the systemic activation of the senescence of the N_2-fixing bacteroids (Fig. 3). At the transcriptional level, these responses correlate with the down-regulation of the leghemoglobin gene family, several transcripts involved in ammonium assimilation, as well as in the rapid up-regulation of the transcripts encoding nodule cysteine proteases and many other plant proteins involved in nodule senescence, including the MtNAC969 transcription factor. Up-regulation of cysteine proteases and MtNAC969 transcripts during nitrate-induced nodule senescence has been previously reported (Pérez Guerra *et al.*, 2010; de Zélicourt *et al.*, 2012; Pierre *et al.*, 2014). This up-regulation does not require the presence of nitrate at the periphery of the nodules *per se*, but is under the control of the nutrient status of the whole plant. Our data are compatible with the hypothesis of nodule senescence being the cause direct of the down-regulation of N_2 fixation, but does not rule out that additional mechanisms may also contribute to this repression. Systemic N-satiety signaling stimulates accumulation of transcripts encoding chitinase, glucanase, and pathogenesis-related proteins, as well as transcripts involved in jasmonic acid biosynthesis (van Loon *et al.*, 2006; Bari and Jones, 2009) that are known components of the pathogen-triggered immunity response generally attenuated during nodule formation (Berrabah *et al.*, 2015; Gourion *et al.*, 2015). The re-activation of defense responses against microorganisms parallels the arrest of the symbiotic association during systemically induced nodule senescence. Systemic N satiety signaling down-regulates the accumulation of numerous transcripts involved in cell division and meristematic activity (cyclin, core histones) as well as transcripts specific to the symbiotic organ development program such as transcripts encoding nodulins, GRPs, and most of the transcripts of the large NCR peptide family. Interestingly, two classes of NCR transcripts are discriminated based on their early or late responses to systemic N-satiety signaling. Diversity within the NCR gene family related to transcript accumulation kinetics, impact on bacteroid differentiation, and host specificity have already been reported (Guefrachi *et al.*, 2014; Kereszt *et al.*, 2018). Whether the differential responses to N-deficit signaling are related to the distinct functions of these peptides remains to be investigated. Previous work has evidenced that the systemic N-deficit signaling has no clear effect on nodule SNF specific activity (SNF per biomass of nodule) but stimulates nodule expansion that finally results in elevating nodule SNF in the long term (SNF per nodule; Ruffel *et al.*, 2008; Jeudy *et al.*, 2010; Laguerre *et al.*, 2012). Although the impact of N-deficit on mature nodule expansion is hardly measurable after 3 d, we observed an early inhibition of bacteroid senescence, an early down-regulation of nodule cysteine protease gene expression, as well as an early stimulation of the accumulation of NCR and GRP peptide transcripts in response to N-deficit systemic signaling. As NCRs and GRPs have been implicated in early and late bacteroid differentiation (Kereszt *et al.*, 2018), these responses may mark the early stimulation of the bacteroid differentiation that has been already characterized as a long-term response to N-deficit signaling (Laguerre *et al.*, 2012). Massive reprogramming was not observed in symbiotic bacteria as the main variations affecting bacterial transcripts were probably indirectly related to the lysis of bacteroids rather to a direct response of bacteroid gene expression to N signaling. Globally the data are consistent with the view of plant systemic N signaling having the driving role in determining mutualism behavior of the mature symbiotic organs. Altogether the data give further support to the model of bacteroid differentiation and persistence being tuned by the plant through activation of defenses and senescence (Berrabah *et al.*, 2015), and further suggest that systemic N signaling pilots these controls. However, at this stage, it cannot be ruled out that variation of genetic expression in bacteroids operates at the post-transcriptional level. A striking example that may argue for post-transcriptional regulation in bacteroids in response to N signaling is the apparent discrepancy between the impact of N-deficit on the 'GABA shunt' activity in mature nodules that is well observed at the level of metabolite accumulation but not associated with clear variation of the accumulation of the transcripts encoding the related enzymes.

Systemic N signaling triggers major variations of the metabolite pools of the mature nodule that are inversely correlated with the whole-plant N demand. They illustrate the variations of the exchanges between nodules and the whole plant. Whole-plant N-satiety and N-deficit signaling, respectively, trigger a dramatic reduction and substantial increase of sugar pools within the first day of treatment. These variations are correlated with changes of the levels of transcripts involved in glycolysis, sucrose metabolism, starch degradation, and biosynthesis. Because most of these responses tend to compensate sugar pool variations, they are likely to be the consequences rather than the cause of changes of the sugar content of the nodule. As the sucrose produced by photosynthesis and translocated from the shoot to the root through the phloem stream is the primary source of nodule carbon metabolites (Udvardi and Poole, 2013; Liu *et al.*, 2018), the sugar pool variations are probably due to changes in the phloem-driven sucrose partitioning from the shoot to the symbiotic organ rather than to nodule metabolism activity. Interestingly, variations in the sugar content of the nodule correlate with variations of the accumulation of several transcripts involved in sugar transport, some encoding SWEET sugar transporters that are potentially involved in the sugar export from the source tissue to the nodule (Kryvoruchko *et al.*, 2016). Variations of assimilate partitioning from the shoot to the nodules have already been correlated with early systemic N-deficit signaling using $^{13}CO_2$ labeling in *M. truncatula* nodulated plants exposed to a local suppression of N_2 fixation (4 d of Ar/O_2 treatment; Jeudy *et al.*, 2010). These N-deficit systemic responses include rapid variation of sugar content of the nodule already measured after 1 d of partial arrest of

SNF. N-satiety is associated with the reduction of the asparagine and glutamate pools produced by the assimilation of the NH_4^+ by SNF, as well as the malate pool, the primary carbon and energy source provided by the plant to the bacteroid (Udvardi and Poole, 2013). N-satiety also reduces the GABA, alanine, and succinic semialdehyde pools that mark the activity of the so-called 'GABA shunt'. This metabolic pathway was suggested to allow the hypoxic symbiotic tissues to maintain the efficiency of the TCA cycle (Prell *et al.*, 2009) and was proposed to be regulated by the plant through GABA partitioning from the shoot to the nodule (Sulieman and Schulze, 2010; Sulieman, 2011). N-deficit signaling mirrors N-satiety systemic responses by increasing these metabolite pools. Amino acids have been suggested as potential signals for systemic N regulation of symbiosis, indicating a specific 'N-feedback' mechanism (Parsons *et al.*, 1993; Bacanamwo and Harper, 1997; Sulieman and Schulze, 2010; Sulieman *et al.*, 2010). Nevertheless, although the levels of many amino acids and some organic acids vary in response to systemic N signaling, their accumulation kinetics are late as compared with sugars, early transcriptome reprogramming, and SNF (in the case of N-satiety). Therefore, the variatons in amino acids and organic acids are more likely to be consequences of sucrose partitioning. Sugar allocation by the plant to the nodule may behave as a systemic metabolic signal that drives nodule function and development. Earlier reports indicated that (i) carbon partitioning is limiting nodule development and function at vegetative stages (Voisin *et al.*, 2003); and (ii) increasing partitioning of photosynthates from the shoot to the roots by elevating ambient CO_2 enhances SNF in legumes (Rogers *et al.*, 2006). Furthermore the role of SWEET transporters in the control of the plant interaction with pathogenic microbes has already been documented (Bezrutczyk *et al.*, 2018). This work suggests that these transporters may also contribute to adjusting the benefits of beneficial microorganisms to plant nutritional demand. However, how the whole-plant N status is perceived in order to modulate sucrose allocation remains to be discovered.

Although the variation of sugar allocation is, to our knowledge, the earliest known response to systemic N signaling in mature nodules, it cannot be excluded that there is a consequence of reprogramming of nodule development by hormonal and/or peptide signals. Systemic N signaling modulates the accumulation of a number of transcripts involved in (i) the CK transduction pathway as well as in CK inactivation and biosynthesis; (ii) ethylene biosynthesis; (iii) jasmonic acid biosynthesis; and (iv) expression of several genes encoding CEP and CLE peptide hormones. All of these hormones and peptides can be mobile signals, have been implicated in the control of nodule formation and development (Ferguson and Mathesius, 2014; Buhian and Bensmihen, 2018), and therefore could be involved in the systemic control of mature nodules. Further investigations are required to discriminate whether these hormones and peptides may be direct systemic signals of N status of the plant or secondary components of the systemic N responses.

This study illustrates that the function and development of the symbiotic organs are highly integrated at the whole-holobiont level. Systemic regulations could be interpreted according to a mutualism model based on plant C–N trade-offs. Plants under N-deficit stimulate SNF by allocating photosynthates toward N_2-fixing mature nodules, whereas when the N demand is satisfied by addition of mineral N the plants shut down this allocation and promote symbiotic organ senescence as the C cost of SNF is excessive as compared with mineral N nutrition. Because of climate change, atmospheric ambient CO_2 is expected to increase, modifying the conditions of symbiotic C–N trade-offs (Rogers *et al.*, 2006). How this may consequently modify the equilibrium of *Rhizobium*–legume mutualism is an open question that deserves further investigation.

Supplementary data

Supplementary data are available at *JXB* online.

Fig. S1. Global view of responses of the mature nodule transcriptome to N signaling.

Fig. S2. Global comparison of the plant transcriptome responses identified in this study with the previous data of Ruffel *et al.* (2008) and Cabeza *et al.* (2014).

Fig. S3. Heat map of transcript accumulation of plant DEGs annotated as cysteine proteases.

Fig. S4. Heat map of transcript accumulation of expressed plant genes annotated as proteases.

Fig. S5. Heat map of transcript accumulation of plant DEGs annotated as plant hemoglobins.

Fig. S6. Heat map of transcript accumulation of plant DEGs annotated as glycine-rich peptides (GRPs).

Fig. S7. Heat map of transcript accumulation of plant DEGs annotated as nodule cysteine-rich (NCR) peptides.

Fig. S8. Heat map of transcript accumulation of expressed plant genes annotated as CLE or CEP peptides.

Fig. S9. Box-plot representation of the relative accumulation of leghemoglobin, cysteine protease, and sweet 11 transcripts in response to systemic N-satiety or N-deficit signaling in three independent split-root experiments.

Table S1. Effect of systemic N signaling on sugar contents of mature nodules.

Table S2. Effect of systemic N signaling on soluble amino acid contents of mature nodules.

Table S3. Effect of systemic N signaling on organic acid contents of mature nodules.

Table S4. RNAseq data of the plant genes expressed in control, DN_2, and SN_2 mature nodules (log_2-normalized counts).

Table S5. Differential expression of N-deficit and N-satiety plant DEG transcripts in the various temporal contrasts of the analysis (DE_groups).

Table S6. Gene Ontology (GO) enrichment comparison between N-satiety and N-deficit plant DEGs.

Table S7. RNAseq data of the bacterial genes expressed in control, DN_2, and SN_2 mature nodules (log_2-normalized counts).

Table S8. Differential expression of N-deficit and N-satiety bacterial DEG transcripts in the various temporal contrasts of the analysis (DE_groups).

Table S9. Assignment of total plant DEGs to co-expression clusters and metaclusters.

Table S10. Preferential expression of the DEGs in the nodule zones deduced from the data of Roux *et al*, 2014.

Table S11. Enrichment in the functional annotation terms of the co-expressed DEGs as compared with their representation in the whole genome (Mtv4.2) by hypergeometric tests.

Acknowledgements

This work was supported by the ANR grants Psyche (ANR-16-CE20-0009-02) and LabEx Saclay Plant Sciences-SPS (ANR-10-LABX-0040-SPS). We thank Stephane Boivin and Clare Cough for critical reading of the manuscript.

Author contributions

ML designed the experiments; MP and ML performed the split-root experiments; MP, ML, and GC performed metabolome analysis; MP, ML, and PT performed ^{15}N labeling and analysis; AL-Q, MP, and CB performed histology analysis; AL-Q, MT, DS, and SC sequenced, assembled, and annotated the MD4 genome; MP and AL-Q performed sample preparation for RNAseq; IL, DS, M-LM-M, SC, and ML performed the RNAseq data production, analysis, and biological interpretation; ML wrote the manuscript with contributions from SC and IL, and revisions of all authors.

References

Azarakhsh M, Lebedeva MA, Lutova LA. 2018. Identification and expression analysis of *Medicago truncatula* Isopentenyl Transferase Genes (IPTs) involved in local and systemic control of nodulation. Frontiers in Plant Science **9**, 304.

Bacanamwo M, Harper JE. 1997. The feedback mechanism of nitrate inhibition of nitrogenase activity in soybean may involve asparagine and/or products of its metabolism. Physiologia Plantarum **100**, 371–377.

Baier MC, Barsch A, Küster H, Hohnjec N. 2007. Antisense repression of the *Medicago truncatula* nodule-enhanced sucrose synthase leads to a handicapped nitrogen fixation mirrored by specific alterations in the symbiotic transcriptome and metabolome. Plant Physiology **145**, 1600–1618.

Bari R, Jones JD. 2009. Role of plant hormones in plant defence responses. Plant Molecular Biology **69**, 473–488.

Becker A, Bergès H, Krol E, *et al*. 2004. Global changes in gene expression in *Sinorhizobium meliloti* 1021 under microoxic and symbiotic conditions. Molecular Plant-Microbe Interactions **17**, 292–303.

Benedito VA, Torres-Jerez I, Murray JD, *et al*. 2008. A gene expression atlas of the model legume *Medicago truncatula*. The Plant Journal **55**, 504–513.

Berrabah F, Ratet P, Gourion B. 2015. Multiple steps control immunity during the intracellular accommodation of rhizobia. Journal of Experimental Botany **66**, 1977–1985.

Bezrutczyk M, Yang J, Eom J-S, *et al*. 2018. Sugar flux and signaling in plant–microbe interactions. The Plant Journal **93**, 675–685.

Breakspear A, Liu C, Roy S, *et al*. 2014. The root hair 'infectome' of *Medicago truncatula* uncovers changes in cell cycle genes and reveals a requirement for auxin signaling in rhizobial infection. The Plant Cell **26**, 4680–4701.

Buhian WP, Bensmihen S. 2018. Nod factor regulation of phytohormone signaling and homeostasis during rhizobia–legume symbiosis. Frontiers in Plant Science **9**, 1247.

Cabeza R, Koester B, Liese R, Lingner A, Baumgarten V, Dirks J, Salinas-Riester G, Pommerenke C, Dittert K, Schulze J. 2014. An RNA sequencing transcriptome analysis reveals novel insights into molecular aspects of the nitrate impact on the nodule activity of *Medicago truncatula*. Plant Physiology **164**, 400–411.

Capela D, Filipe C, Bobik C, Batut J, Bruand C. 2006. *Sinorhizobium meliloti* differentiation during symbiosis with alfalfa: a transcriptomic dissection. Molecular Plant-Microbe Interactions **19**, 363–372.

Clément G, Moison M, Soulay F, Reisdorf-Cren M, Masclaux-Daubresse C. 2018. Metabolomics of laminae and midvein during leaf senescence and source–sink metabolite management in *Brassica napus* L. leaves. Journal of Experimental Botany **69**, 891–903.

Darling AC, Mau B, Blattner FR, Perna NT. 2004. Mauve: multiple alignment of conserved genomic sequence with rearrangements. Genome Research **14**, 1394–1403.

de Zélicourt A, Diet A, Marion J, Laffont C, Ariel F, Moison M, Zahaf O, Crespi M, Gruber V, Frugier F. 2012. Dual involvement of a *Medicago truncatula* NAC transcription factor in root abiotic stress response and symbiotic nodule senescence. The Plant Journal **70**, 220–230.

Dillies MA, Rau A, Aubert J, *et al*. 2013. A comprehensive evaluation of normalization methods for Illumina high-throughput RNA sequencing data analysis. Briefings in Bioinformatics **14**, 671–683.

Durand JL, Sheehy JE, Minchin FR. 1987. Nitrogenase activity, photosynthesis and nodule water potential in soyabean plants experiencing water deprivation. Journal of Experimental Botany **38**, 311–321.

El Yahyaoui F, Küster H, Ben Amor B, *et al*. 2004. Expression profiling in *Medicago truncatula* identifies more than 750 genes differentially expressed during nodulation, including many potential regulators of the symbiotic program. Plant Physiology **136**, 3159–3176.

Ferguson BJ, Mathesius U. 2014. Phytohormone regulation of legume–rhizobia interactions. Journal of Chemical Ecology **40**, 770–790.

Ferguson BJ, Mens C, Hastwell AH, Zhang M, Su H, Jones CH, Chu X, Gresshoff PM. 2019. Legume nodulation: the host controls the party. Plant, Cell & Environment **42**, 41–51.

Fiehn O. 2006. Metabolite profiling in Arabidopsis. Methods in Molecular Biology **323**, 439–447.

Gil-Quintana E, Larrainzar E, Arrese-Igor C, González EM. 2013. Is N-feedback involved in the inhibition of nitrogen fixation in drought-stressed *Medicago truncatula*? Journal of Experimental Botany **64**, 281–292.

González EM, Gordon AJ, James CL, Arrese-Igor C. 1995. The role of sucrose synthase in the response of soybean nodules to drought. Journal of Experimental Botany **46**, 1515–1523.

Gourion B, Berrabah F, Ratet P, Stacey G. 2015. *Rhizobium*–legume symbioses: the crucial role of plant immunity. Trends in Plant Science **20**, 186–194.

Guefrachi I, Nagymihaly M, Pislariu CI, Van de Velde W, Ratet P, Mars M, Udvardi MK, Kondorosi E, Mergaert P, Alunni B. 2014. Extreme specificity of NCR gene expression in *Medicago truncatula.* BMC genomics **15**, 712.

Guinel FC. 2015. Ethylene, a hormone at the center-stage of nodulation. Frontiers in Plant Science **6**, 1121.

Huault E, Laffont C, Wen J, Mysore KS, Ratet P, Duc G, Frugier F. 2014. Local and systemic regulation of plant root system architecture and symbiotic nodulation by a receptor-like kinase. PLoS Genetics **10**, e1004891.

Hunt S, Layzell DB. 1993. Gas exchange of legume nodules and the regulation of nitrogenase activity. Annual Review of Plant Physiology and Plant Molecular Biology **44**, 483–511.

Jeudy C, Ruffel S, Freixes S, *et al*. 2010. Adaptation of *Medicago truncatula* to nitrogen limitation is modulated via local and systemic nodule developmental responses. New Phytologist **185**, 817–828.

Kereszt A, Mergaert P, Montiel J, Endre G, Kondorosi É. 2018. Impact of plant peptides on symbiotic nodule development and functioning. Frontiers in Plant Science **9**, 1026.

Kinkema M, Gresshoff PM. 2008. Investigation of downstream signals of the soybean autoregulation of nodulation receptor kinase GmNARK. Molecular Plant-Microbe Interactions **21**, 1337–1348.

Kosslak RM, Bohlool BB. 1984. Suppression of nodule development of one side of a split-root system of soybeans caused by prior inoculation of the other side. Plant Physiology **75**, 125–130.

Kryvoruchko IS, Sinharoy S, Torres-Jerez I, Sosso D, Pislariu CI, Guan D, Murray J, Benedito VA, Frommer WB, Udvardi MK. 2016.

MtSWEET11, a nodule-specific sucrose transporter of *Medicago truncatula*. Plant Physiology **171**, 554–565.

Laffont C, Huault E, Gautrat P, Endre G, Kalo P, Bourion V, Duc G, Frugier F. 2019. Independent regulation of symbiotic nodulation by the SUNN negative and CRA2 positive systemic pathways. Plant Physiology **180**, 559–570.

Laguerre G, Heulin-Gotty K, Brunel B, Klonowska A, Le Quéré A, Tillard P, Prin Y, Cleyet-Marel JC, Lepetit M. 2012. Local and systemic N signaling are involved in *Medicago truncatula* preference for the most efficient *Sinorhizobium* symbiotic partners. The New Phytologist **195**, 437–449.

Li Y, Krouk G, Coruzzi GM, Ruffel S. 2014. Finding a nitrogen niche: a systems integration of local and systemic nitrogen signalling in plants. Journal of Experimental Botany **65**, 5601–5610.

Libault M, Farmer A, Brechenmacher L, *et al*. 2010. Complete transcriptome of the soybean root hair cell, a single-cell model, and its alteration in response to *Bradyrhizobium japonicum* infection. Plant Physiology **152**, 541–552.

Liu A, Contador CA, Fan K, Lam HM. 2018. Interaction and regulation of carbon, nitrogen, and phosphorus metabolisms in root nodules of legumes. Frontiers in Plant Science **9**, 1860.

Lodwig EM, Hosie AH, Bourdès A, Findlay K, Allaway D, Karunakaran R, Downie JA, Poole PS. 2003. Amino-acid cycling drives nitrogen fixation in the legume–*Rhizobium* symbiosis. Nature **422**, 722–726.

Lohar DP, Sharopova N, Endre G, Peñuela S, Samac D, Town C, Silverstein KA, VandenBosch KA. 2006. Transcript analysis of early nodulation events in *Medicago truncatula*. Plant Physiology **140**, 221–234.

Luo R, Liu B, Xie Y, *et al*. 2012. SOAPdenovo2: an empirically improved memory-efficient short-read de novo assembler. GigaScience **1**, 18.

Mitra RM, Long SR. 2004. Plant and bacterial symbiotic mutants define three transcriptionally distinct stages in the development of the *Medicago truncatula*/*Sinorhizobium meliloti* symbiosis. Plant Physiology **134**, 595–604.

Moreau S, Verdenaud M, Ott T, Letort S, de Billy F, Niebel A, Gouzy J, de Carvalho-Niebel F, Gamas P. 2011. Transcription reprogramming during root nodule development in *Medicago truncatula*. PLoS One **6**, e16463.

Mortier V, De Wever E, Vuylsteke M, Holsters M, Goormachtig S. 2012. Nodule numbers are governed by interaction between CLE peptides and cytokinin signaling. The Plant Journal **70**, 367–376.

Nakagawa T, Kawaguchi M. 2006. Shoot-applied MeJA suppresses root nodulation in *Lotus japonicus*. Plant & Cell Physiology **47**, 176–180.

Okamoto S, Tabata R, Matsubayashi Y. 2016. Long-distance peptide signaling essential for nutrient homeostasis in plants. Current Opinion in Plant Biology **34**, 35–40.

Oldroyd GE, Murray JD, Poole PS, Downie JA. 2011. The rules of engagement in the legume–rhizobial symbiosis. Annual Review of Genetics **45**, 119–144.

Olsson JE, Nakao P, Bohlool BB, Gresshoff PM. 1989. Lack of systemic suppression of nodulation in split root systems of supernodulating soybean (*Glycine max* [L.] Merr.) mutants. Plant Physiology **90**, 1347–1352.

Parsons R, Stanforth A, Raven JA, Sprent JI. 1993. Nodule growth and activity may be regulated by a feedback mechanism involving phloem nitrogen. Plant, Cell & Environment **16**, 125–136.

Pecrix Y, Staton SE, Sallet E, *et al*. 2018. Whole-genome landscape of *Medicago truncatula* symbiotic genes. Nature Plants **4**, 1017–1025.

Pérez Guerra JC, Coussens G, De Keyser A, De Rycke R, De Bodt S, Van De Velde W, Goormachtig S, Holsters M. 2010. Comparison of developmental and stress-induced nodule senescence in *Medicago truncatula*. Plant Physiology **152**, 1574–1584.

Pierre O, Hopkins J, Combier M, Baldacci F, Engler G, Brouquisse R, Hérouart D, Boncompagni E. 2014. Involvement of papain and legumain proteinase in the senescence process of *Medicago truncatula* nodules. New Phytologist **202**, 849–863.

Prell J, Bourdès A, Karunakaran R, Lopez-Gomez M, Poole P. 2009. Pathway of gamma-aminobutyrate metabolism in *Rhizobium leguminosarum* 3841 and its role in symbiosis. Journal of Bacteriology **191**, 2177–2186.

Rau A, Maugis-Rabusseau C. 2018. Transformation and model choice for RNA-seq co-expression analysis. Briefings in Bioinformatics **19**, 425–436.

Reid D, Liu H, Kelly S, Kawaharada Y, Mun T, Andersen SU, Desbrosses G, Stougaard J. 2018. Dynamics of ethylene production in response to compatible Nod factor. Plant Physiology **176**, 1764–1772.

Robinson MD, McCarthy DJ, Smyth GK. 2010. edgeR: a Bioconductor package for differential expression analysis of digital gene expression data. Bioinformatics **26**, 139–140.

Rogers A, Gibon Y, Stitt M, Morgan PB, Bernacchi CJ, Ort DR, Long SP. 2006. Increased C availability at elevated carbon dioxide concentration improves N assimilation in a legume. Plant, Cell & Environment **29**, 1651–1658.

Roux B, Rodde N, Jardinaud M-F, *et al*. 2014. An integrated analysis of plant and bacterial gene expression in symbiotic root nodules using laser-capture microdissection coupled to RNA sequencing. The Plant Journal **77**, 817–837.

Ruffel S, Freixes S, Balzergue S, *et al*. 2008. Systemic signaling of the plant nitrogen status triggers specific transcriptome responses depending on the nitrogen source in *Medicago truncatula*. Plant Physiology **146**, 2020–2035.

Rutten PJ, Poole PS. 2019. Oxygen regulatory mechanisms of nitrogen fixation in rhizobia. Advances in Microbial Physiology **75**, 325–389.

Sallet E, Roux B, Sauviac L, *et al*. 2013. Next-generation annotation of prokaryotic genomes with EuGene-P: application to *Sinorhizobium meliloti* 2011. DNA Research **20**, 339–354.

Sasaki T, Suzaki T, Soyano T, Kojima M, Sakakibara H, Kawaguchi M. 2014. Shoot-derived cytokinins systemically regulate root nodulation. Nature Communications **5**, 4983.

Schwember AR, Schulze J, del Pozo A, Cabeza RA. 2019. Regulation of symbiotic nitrogen fixation in legume root nodules. Plants **8**, 333.

Serraj R, Sinclair TR, Purcell LC. 1999. Symbiotic N_2 fixation response to drought. Journal of Experimental Botany **50**, 143–155.

Sheehy JE, Minchin FR, Witty JF. 1983. Biological control of the resistance to oxygen flux in nodules. Annals of Botany **52**, 565–571.

Streeter J, Wong PP. 1988. Inhibition of legume nodule formation and N_2 fixation by nitrate. Critical Reviews in Plant Sciences **7**, 1–23.

Sugiyama A, Saida Y, Yoshimizu M, Takanashi K, Sosso D, Frommer WB, Yazaki K. 2017. Molecular characterization of LjSWEET3, a sugar transporter in nodules of *Lotus japonicus*. Plant & Cell Physiology **58**, 298–306.

Sulieman S. 2011. Does GABA increase the efficiency of symbiotic N_2 fixation in legumes? Plant Signaling & Behavior **6**, 32–36.

Sulieman S, Fischinger SA, Gresshoff PM, Schulze J. 2010. Asparagine as a major factor in the N-feedback regulation of N_2 fixation in *Medicago truncatula*. Physiologia Plantarum **140**, 21–31.

Sulieman S, Schulze J. 2010. Phloem-derived γ-aminobutyric acid (GABA) is involved in upregulating nodule N_2 fixation efficiency in the model legume *Medicago truncatula*. Plant, Cell & Environment **33**, 2162–2172.

Taleski M, Imin N, Djordjevic MA. 2018. CEP peptide hormones: key players in orchestrating nitrogen-demand signalling, root nodulation, and lateral root development. Journal of Experimental Botany **69**, 1829–1836.

Tian T, Liu Y, Yan H, You Q, Yi X, Du Z, Xu W, Su Z. 2017. agriGO v2.0: a GO analysis toolkit for the agricultural community, 2017 update. Nucleic Acids Research **45**, W122–W129.

Udvardi MK, Day DA. 1997. Metabolite transport across symbiotic membranes of legume nodules. Annual Review of Plant Physiology and Plant Molecular Biology **48**, 493–523.

Udvardi M, Poole PS. 2013. Transport and metabolism in legume–rhizobia symbioses. Annual Review of Plant Biology **64**, 781–805.

Urbanczyk-Wochniak E, Sumner LW. 2007. MedicCyc: a biochemical pathway database for *Medicago truncatula*. Bioinformatics **23**, 1418–1423.

Vallenet D, Calteau A, Cruveiller S, *et al*. 2017. MicroScope in 2017: an expanding and evolving integrated resource for community expertise of microbial genomes. Nucleic Acids Research **45**, D517–D528.

van Loon LC, Rep M, Pieterse CM. 2006. Significance of inducible defense-related proteins in infected plants. Annual Review of Phytopathology **44**, 135–162.

van Wyk SG, Du Plessis M, Cullis CA, Kunert KJ, Vorster BJ. 2014. Cysteine protease and cystatin expression and activity during soybean nodule development and senescence. BMC Plant Biology **14**, 294.

Voisin AS, Salon C, Jeudy C, Warembourg FR. 2003. Symbiotic N_2 fixation activity in relation to C economy of *Pisum sativum* L. as a function of plant phenology. Journal of Experimental Botany **54**, 2733–2744.

Zerbino DR, Birney E. 2008. Velvet: algorithms for de novo short read assembly using de Bruijn graphs. Genome Research **18**, 821–829.